Surface enhanced Raman optical activity (SEROA)

Salim Abdali[a] and Ewan William Blanch*[b]

Received 22nd February 2008
First published as an Advance Article on the web 18th March 2008
DOI: 10.1039/b707862p

Raman optical activity (ROA) directly monitors the stereochemistry of chiral molecules and is now an incisive probe of biomolecular structure. ROA spectra contain a wealth of information on tertiary folding, secondary structure and even the orientation of individual residues in proteins and nucleic acids. Extension of ROA to an even wider range of samples could be facilitated by coupling its structural sensitivity to the low-concentration sensitivity provided by plasmon resonance enhancement. This leads to the new technique of surface enhanced ROA, or SEROA, which is complementary to both SERS and ROA. In this *tutorial review*, we present a survey of theoretical and experimental work undertaken to develop SEROA and discuss these efforts in the context of the ROA technique, and, based on the authors' work, outline possible future directions of research for this novel chiroptical spectroscopy.

1. Introduction

Raman optical activity (ROA), which refers to a small difference in the intensity of Raman scattering from chiral molecules in right- and left-circularly polarized incident light or, equivalently, a small circularly polarized component in the scattered light, is a vibrational spectroscopic technique with great potential in biology.[1,2] Although ROA is still far less widely used than conventional Raman spectroscopy, this chirally-sensitive vibrational spectroscopy is now enjoying rapid growth in both the number of practitioners and applications. However, an unavoidable problem has been the weakness of the ROA effect, with ROA scattering intensities being 3–5 orders of magnitude smaller than those of the parent Raman scattering, which leads to the requirements of higher sample concentrations and longer data collection periods. An obviously attractive approach to reducing these sampling requirements and so widen the applicability of ROA is to combine it with plasmon resonance enhancement. Following the precedent of surface enhanced Raman spectroscopy, or SERS, this leads to the new technique of surface enhanced Raman optical activity, or SEROA. In this *tutorial review* we discuss theoretical as well as experimental work reported to date in this endeavour, and though only a small body of literature has appeared so far, considerable interest has been generated. As ROA is still not well known to most SERS spectroscopists, we provide a brief overview of the conventional ROA technique and its application to biology. Recent work from our laboratories on SEROA will be presented, and we will conclude by discussing our thoughts on the future possibilities and challenges of this novel addition to the SERS family.

Since the first reported incidence of the SERS effect[3] and the independent recognition of its origin by two different research groups,[4,5] SERS has enjoyed an exciting, and sometimes turbulent, history. Although there is still much ongoing research into

[a] *Quantum Protein Centre (QUP), Department of Physics, Technical University of Denmark, Lyngby DK-2800, Denmark*
[b] *Manchester Interdisciplinary Biocentre & Faculty of Life Sciences, University of Manchester, 131 Princess Street, Manchester, UK M1 7DN. E-mail: E.Blanch@manchester.ac.uk*

Salim Abdali

Dr Salim Abdali obtained his PhD from Dept of Physics, Technical University of Denmark (DTU). As a spectroscopist, he has employed X-rays, TEM, SEM, AFM and microwaves for optical nano-multilayers for satellite telescope. In 2001 he joined the Quantum Protein Centre as associate professor at DTU, where his work has focused on vibrational optical activity for biomolecular studies, mainly using Raman and ROA combined with SERS. Recently, with co-workers, they have published the developments of SEROA on different molecules, e.g., *myoglobin and cytochrome c.*

Ewan Blanch

Ewan Blanch completed his BSc in chemistry (1991) and a PhD in physical chemistry (1996) from the University of New England in Australia, measuring electric properties of molecules in the lab of Geoff Ritchie. He then undertook postdoctoral research with Laurence Barron and Lutz Hecht in Glasgow developing ROA spectroscopy and in 2003 took up a lectureship in the Department of Biomolecular Sciences at UMIST, now the Manchester Interdisciplinary Biocentre and Faculty of Life Sciences at The University of Manchester.

the underlying mechanisms responsible for this effect, SERS has developed into a range of techniques and a wide variety of applications. This is, of course, due to the almost universal attraction of high sensitivity that can arise from plasmon resonances generated by certain metal surfaces. Selective enhancements of specific Raman signals over conventional scattering intensities are widely documented in the literature with typical enhancements of 10^3–10^6 and maximum enhancements of up to 10^{14} being reported.[6,7] Such high sensitivity, coupled with selectivity to particular surfaces, has led to SERS being widely used in the analytical sciences, chemistry, biology, medical diagnostics, nanolithography and elsewhere, as this issue of *Chemical Society Reviews* testifies. Further descriptions of SERS and its manifold uses lie beyond the scope of this review, in which we will concentrate specifically on its application to another derivative of Raman spectroscopy, ROA.

1.1. History of SEROA

The enhancement of ROA signals from chiral molecules adsorbed onto metal surfaces was first considered in the literature by Efrima who predicted that these measurements could contain information on both the target molecule and "local electric fields, their gradients and, in general, local dielectric properties of the metal–air (or metal–solution) interface".[8] Efrima developed the first theoretical treatment of the metal surface enhancement of ROA bands in a more extensive paper soon afterwards.[9] Hecht and Barron[10,11] later developed expressions for ROA scattering, as well as for the case of linearly polarized difference Raman scattering, from chiral molecules on isotropic surfaces, including contributions from anti-symmetric contributions of polarizability tensor components for the first time. The authors suggested that ROA may be a promising technique for probing the chirality of metal surfaces.

Despite these pioneering papers that began to explore the mechanisms of ROA in the vicinity of metal surfaces, experimental progress was slow. Initial attempts to measure SEROA were subject to experimental problems. In the last few years there has been a resurgence in research into SEROA as the number of groups using ROA has begun to increase more rapidly. It is indicative of the potential benefits of combining surface enhancement methods with ROA that in private communications many of these new ROA researchers have expressed interest in conducting research into SEROA. The most extensive theoretical formalism of SEROA so far has been presented by Janesko and Scuseria[12] who considered the effects of orientational averaging for the first time, and include the first published calculations of SEROA spectra, for (*R*)-(−)-bromochlorofluoromethane. The first purported SEROA measurements have also recently been published. Following an introduction to the ROA technique we will discuss the research conducted to date, including previously unpublished work from the authors' laboratories, into SEROA in greater detail.

2. Conventional ROA spectroscopy

In 1969, a general theory of the polarization characteristics of Rayleigh and Raman scattered light from chiral molecules was presented by Atkins and Barron.[13] This theory led to the prediction that "the scattered light carries a very small degree of circular polarization and the scattered intensity is slightly different in right- and left-circular polarized incident light" and the new chiroptical technique of Raman optical activity, also known as ROA, was born. Barron and Buckingham in 1971 introduced the dimensionless circular intensity difference (CID) as an appropriate experimental observable[14] and which is defined as

$$\Delta = \frac{(I^{R} - I^{L})}{(I^{R} + I^{L})} \tag{1}$$

where I^{R} and I^{L} are the Raman scattering intensities in right- and left-circularly polarized incident light, respectively. The earliest attempts to measure ROA faced major challenges as the effect is weak, with values of Δ being of the order of 10^{-3} of the conventional Raman effect at the greatest, and pushed the technology available at the time to the limit. Several early published ROA spectra were found to be spurious as ROA measurements are highly sensitive to artefacts. It was not until 1973 that the first reliable ROA spectra were reported[15] and these results were confirmed soon afterwards by Hug *et al.*[16] Although the ROA technique was limited to only a handful of laboratories until recently, it has proven to be a powerful probe of stereochemistry and molecular structure. The success of biomolecular studies has generated the recent increase in the number of ROA researchers and the scope of applications. Examples of ROA studies of biomolecules will be presented below for the benefit of readers not familiar with this technique, but more thorough reviews may be found elsewhere.[17,18]

2.1. The ROA observables, polarizability and optical activity tensors

Scattered light, within a semiclassical treatment, originates from the characteristic radiation fields generated by the oscillating electric and magnetic multipole moments induced in a molecule by the incident light wave. In Cartesian tensor notation, the electric dipole (μ_α), magnetic dipole (m_α) and traceless electric quadrupole moments ($\Theta_{\alpha\beta}$) are respectively defined as[1]

$$\mu_\alpha = \sum_i e_i r_{i_\alpha} \tag{2}$$

$$m_\alpha = \sum_i \frac{e_i}{2m_i} \varepsilon_{\alpha\beta\gamma} r_{i_\beta} p_{i_\gamma} \tag{3}$$

$$\Theta_{\alpha\beta} = \tfrac{1}{2} \sum_i e_i (3 r_{i_\alpha} r_{i_\beta} - r_i^2 \delta_{\alpha\beta}) \tag{4}$$

where particle i at r_i has charge e_i, mass m_i and linear momentum p_i. The real oscillating electric dipole, magnetic dipole and electric quadrupole moments induced in a molecule by the real part of an electric field vector of plane-wave light are, in the far from resonance approximation,

$$\mu_\alpha = \alpha_{\alpha\beta} E_\beta + \frac{1}{\omega} G'_{\alpha\beta} \dot{B}_\beta + \frac{1}{3} A_{\alpha\beta\gamma} \nabla_\beta E_\gamma + \cdots \tag{5}$$

$$m_\alpha = -\frac{1}{\omega} G'_{\alpha\beta} \dot{E}_\beta + \cdots \tag{6}$$

$$\Theta_{\alpha\beta} = A_{\alpha\beta\gamma} E_\gamma + \cdots \tag{7}$$

where B_α is the associated magnetic vector and $\nabla_\alpha E_\beta$ is the electric field gradient.

Evaluation of the fields and field gradients at the same molecular origin used to define the molecular multipole moments gives the following quantum mechanical expressions for the dynamic molecular property tensors using time-dependent perturbation theory[17]

$$\alpha_{\alpha\beta} = \frac{2}{\hbar}\sum_{j\neq n}\frac{\omega_{jn}}{\omega_{jn}^2-\omega^2}\mathrm{Re}(\langle n|\mu_\alpha|j\rangle\langle j|\mu_\beta|n\rangle) \quad (8)$$

$$G'_{\alpha\beta} = -\frac{2}{\hbar}\sum_{j\neq n}\frac{\omega}{\omega_{jn}^2-\omega^2}\mathrm{Im}(\langle n|\mu_\alpha|j\rangle\langle j|m_\beta|n\rangle) \quad (9)$$

$$A_{\alpha\beta\gamma} = \frac{2}{\hbar}\sum_{j\neq n}\frac{\omega_{jn}}{\omega_{jn}^2-\omega^2}\mathrm{Re}(\langle n|\mu_\alpha|j\rangle\langle j|\Theta_{\beta\gamma}|n\rangle) \quad (10)$$

In the above expressions, n and j are the initial and virtual intermediate states of the molecule, respectively, and $\omega_{jn} = \omega_j - \omega_n$ is their angular frequency separation. The electric dipole–electric dipole tensor $\alpha_{\alpha\beta}$ is simply the polarizability responsible for conventional Raman scattering and many other optical effects, $G'_{\alpha\beta}$ is the electric dipole–magnetic dipole optical activity tensor whose isotropic component is responsible for optical rotation in fluids, and $A_{\alpha\beta\gamma}$ is the electric dipole–electric quadrupole tensor responsible for additional contributions to optical rotation in oriented samples.

We can consider the form of the ROA observables as a function of the experimental scattering geometry. In terms of the polarizability and optical activity tensors defined in eqn (8)–(10), the CID expressions for forward (0°) and backward (180°) scattering geometries, for isotropic samples and incident wavelengths much greater than the molecular dimensions, are[1,17]

$$\Delta(0^\circ) = \frac{4[45\alpha G' + \beta(G')^2 - \beta(A)^2]}{c[45\alpha^2 + 7\beta(\alpha)^2]} \quad (11)$$

$$\Delta(180^\circ) = \frac{24[\beta(G')^2 + \tfrac{1}{3}\beta(A)^2]}{c[45\alpha^2 + 7\beta(\alpha)^2]} \quad (12)$$

where the isotropic invariants of the polarizability tensor and the electric dipole–magnetic dipole optical activity tensor are defined as

$$\alpha = \tfrac{1}{3}\alpha_{\alpha\alpha} = \tfrac{1}{3}(\alpha_{xx} + \alpha_{yy} + \alpha_{zz}) \quad (13)$$

$$G' = \tfrac{1}{3}G'_{\alpha\alpha} = \tfrac{1}{3}(G'_{xx} + G'_{yy} + G'_{zz}) \quad (14)$$

and the anisotropic invariants of the polarizability–polarizability and polarizability–optical activity tensor component products are defined as

$$\beta(\alpha)^2 = \tfrac{1}{2}(3\alpha_{\alpha\beta}\alpha_{\alpha\beta} - \alpha_{\alpha\alpha}\alpha_{\beta\beta}) \quad (15)$$

$$\beta(G')^2 = \tfrac{1}{2}(3\alpha_{\alpha\beta}G'_{\alpha\beta} - \alpha_{\alpha\alpha}G'_{\beta\beta}), \quad (16)$$

$$\beta(A)^2 = \tfrac{1}{2}\omega\alpha_{\alpha\beta}\varepsilon_{\alpha\gamma\delta}A_{\gamma\delta\beta} \quad (17)$$

For a molecule composed entirely of idealized axially symmetric bonds, for which $\beta(G')^2 = \beta(A)^2$ and $\alpha G' = 0$ (ref. 1 and references cited therein), a simple bond polarizability model finds that ROA is generated exclusively by anisotropic scattering and the CID expressions reduce to

$$\Delta(0^\circ) = 0, \quad (18)$$

$$\Delta(180^\circ) = \frac{32\beta(G')^2}{c[45\alpha^2 + 7\beta(\alpha)^2]} \quad (19)$$

Therefore, unlike the case of conventional Raman scattering, in which intensities are the same in all directions, ROA intensities are maximized in backscattering and are zero in forwardscattering. The equations presented above were originally formulated for incident circular polarization, or ICP, ROA. The ROA effect is also manifest as a small circularly polarized component in the scattered light, with this being known as scattered circular polarization ROA, or SCP ROA. Within the far-from-resonance approximation, SCP ROA provides equivalent information to ICP ROA, and these two ROA scattering mechanisms are illustrated in Fig. 1. A commercial ROA spectrometer now available employs the SCP measurement strategy.[19] Simultaneous measurement of both ICP and SCP ROA, which is called dual circular polarization (DCP) ROA, can also be undertaken.[20] Although leading research is still being undertaken with ICP ROA spectrometers, most ROA studies are now being conducted with SCP ROA instruments. In SCP ROA, the right- and left-circular scattered intensities are denoted as I_R and I_L, respectively.

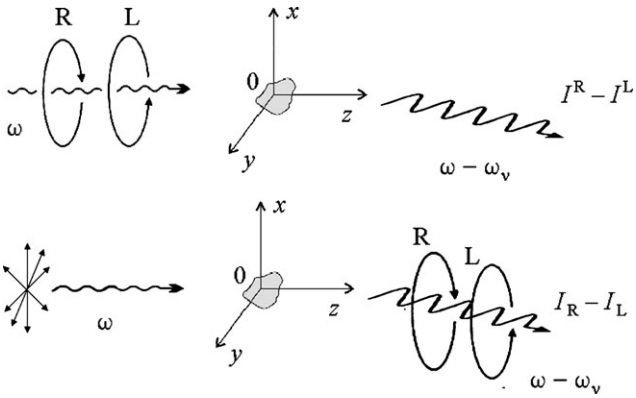

Fig. 1 Representations of ICP (upper) and SCP (lower) ROA experiments from Stokes Raman scattering at angular frequency $\omega - \omega_\nu$ in incident light with angular frequency ω. ICP ROA spectra are measured as $I^R - I^L$, where I^R and I^L are the scattered intensities, here represented as unpolarized, in right- and left-circularly polarized incident light, respectively. SCP ROA spectra are measured as $I_R - I_L$, where I_R and I_L are the intensities of the right- and left-circularly polarized components of the scattered light, respectively, measured with, in this case, unpolarized incident light. At transparent frequencies ICP ROA and SCP ROA are equivalent.

2.2. Instrumentation

As discussed above, ROA is maximized in backscattering and this geometry is essential for the routine measurement of ROA spectra of biomolecules in aqueous solution. Until recently, all ROA spectra of biomolecules had been recorded using the ICP design. For a comprehensive account of ICP ROA spectrometer design we direct the reader to ref. 17 and 18 and

references cited therein. In the last few years, the ICP ROA design has been superseded by an SCP design developed by Hug and employing a 'virtual enantiomers' approach.[19] The ICP- and SCP-type ROA spectrometers currently in use all generally rely on excitation at 532 nm and produce spectra that are virtually identical. Recently, a SCP ROA spectrometer has been built that utilises near infrared excitation at 780 nm.[21] The use of NIR excitation may allow investigation of the SEROA phenomenon using gold substrates rather than the silver colloids investigated so far. Dual circular polarization ROA spectroscopy has been less widely exploited.

2.3. ROA spectra of proteins

The typical features found for ROA spectra of proteins and RNAs are briefly described here as a guide to the reader. In the case of proteins, vibrations of the peptide backbone are generally associated with three main regions of the Raman spectrum.[22] The backbone skeletal stretch region $\sim$870–1150 cm^{-1} originates in C_α–C, C_α–C_β and C_α–N stretch coordinates; the extended amide III region $\sim$1230–1340 cm^{-1} arises from mainly the in-phase combination of the N–H in-plane deformation with the C_α–N stretch along with mixing between the N–H and C_α–H deformations; and the amide I region $\sim$1630–1700 cm^{-1} originates in the C=O stretch. Of particular importance in protein ROA spectra is the extended amide III region as coupling between the N–H and C_α–H deformations is sensitive to geometry and this results in a rich and informative band structure.

We present in Fig. 2 the ROA, and corresponding Raman, spectra for three structurally distinct proteins as an example of the sensitivity of ROA spectra to protein structure. More detailed reviews of this subject can be found elsewhere.[18,22] Fig. 2 shows the backscattered Raman (top of first pair) and ROA (bottom of first pair) spectra of the α-helical protein human serum albumin (HSA).[22] The main features of the ROA spectrum are in good agreement with the Protein Data Bank (PDB) X-ray crystal structure 1ao6; 69.2% α-helix, 1.7% 3_{10}-helix and the remainder consisting of loops and turns. The strong sharp positive band at $\sim$1340 cm^{-1} is assigned to a hydrated form of α-helix while the weaker positive band at $\sim$1300 cm^{-1} appears to be associated with α-helix in a more hydrophobic environment. Relative intensities of these two bands correlate with the exposure of the polypeptide backbone to the solvent within the elements of α-helix in each case. The amide I ROA couplet, which is negative at $\sim$1641 cm^{-1} and positive at $\sim$1665 cm^{-1}, is also characteristic of α-helix and corresponds to the range $\sim$1645–1655 cm^{-1} for α-helix bands in conventional Raman spectra. Positive ROA bands in the region $\sim$870–950 cm^{-1} are another signature of α-helix with the detailed band structure in this region appearing to show a dependence upon side chain composition, helix length and the presence of irregularities.

Beneath the HSA spectra in Fig. 2 are shown the Raman and ROA spectra of the β-barrel protein bovine β-lactoglobulin at pH 8.0, which contains, according to the PDB X-ray crystal structure 1beb, 42.3% β-strand, 9.6% α-helix and 6.4% 3_{10}-helix with the remainder being hairpin bends and long loops. The features of this spectrum are obviously very

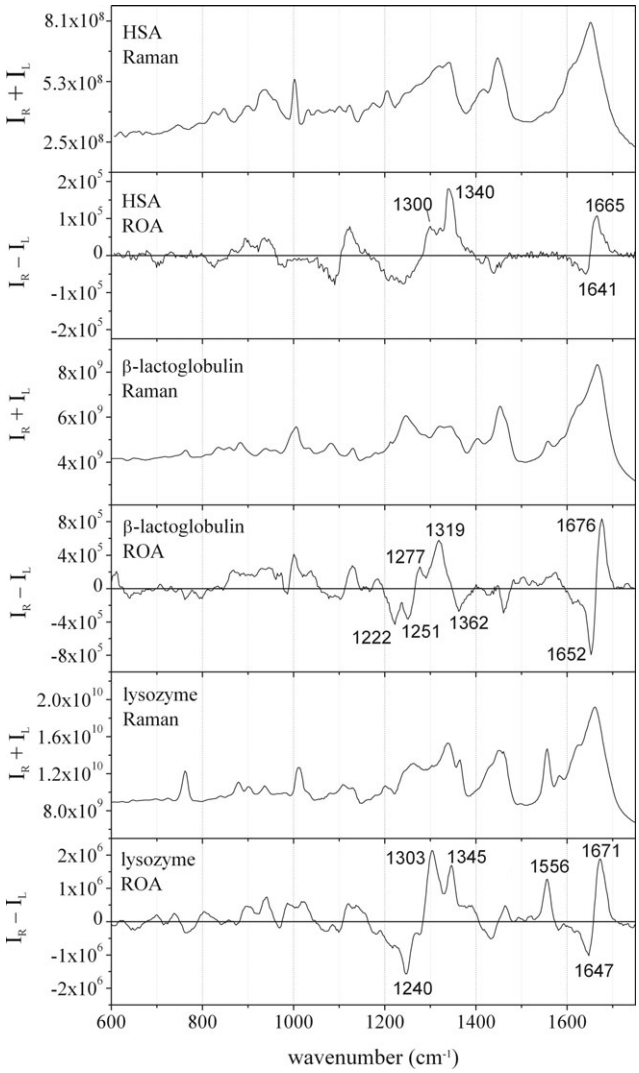

Fig. 2 Backscattered Raman ($I_R + I_L$, upper of each pair) and ROA ($I_R - I_L$, lower of each pair) spectra for human serum albumin (HSA, top), β-lactoglobulin (middle) and hen lysozyme (bottom).

different to those in the ROA spectrum of the α-helical protein HSA, far more so than for the corresponding Raman spectra. The two negative bands at $\sim$1222 cm^{-1} and $\sim$1251 cm^{-1} are characteristic of β-sheet structure. Amide III bands from β-sheet in conventional Raman spectroscopy are assigned to the region $\sim$1230–1245 cm^{-1}. The amide I couplet, negative at $\sim$1652 cm^{-1} and positive at $\sim$1676 cm^{-1}, is another signature of β-sheet and is easily distinguished from the amide I couplet produced by α-helix, which usually occurs $\sim$5–20 cm^{-1} lower. A negative ROA band observed at $\sim$1362 cm^{-1} is assigned to β-hairpins while the positive ROA band at $\sim$1319 cm^{-1} is associated with a distinct form of disordered structure called polyproline II helix. Coappearance of these bands with the β-sheet bands already mentioned is indicative of the antiparallel β-sheet structure of β-lactoglobulin.

Fig. 2 also displays the Raman and ROA spectra of the α + β protein hen lysozyme. The fold of this protein is very different to those of HSA and β-lactoglobulin and this is evident in the large differences between their ROA spectra.

According to the PDB X-ray crystal structure 1lse, hen lysozyme contains 28.7% α-helix, 10.9% 3_{10}-helix and 6.2% β-sheet, which is consistent with the positive ROA bands assigned to hydrophobic and hydrated α-helix at ~1303 and 1345 cm^{-1}, respectively, as well as the sharp negative band ~1240 cm^{-1} from β-structure. There may also be bands contributing in this region from turns. The amide I couplet, negative at ~1647 and positive at 1671 cm^{-1}, also indicates a significant amount of α-helix with a smaller β-sheet component. There is also a small couplet, negative at ~1433 cm^{-1} and positive at ~1463 cm^{-1}, from CH_2 and CH_3 side chain deformations. A relatively large positive band ~1556 cm^{-1} is assigned to the W3-type vibrational mode of the indole ring of tryptophan residues. The position, intensity and sign of this ROA band is sensitive to the torsion angle $\chi^{2,1}$ of the tryptophan side chain, which describes the orientation of the indole ring with respect to the local peptide backbone. Therefore, the absolute stereochemistry of the tryptophan side chain can be directly determined from ROA spectra.[18] This information is not usually available except from a structure determined at atomic resolution.

2.4. RNA spectra

Ribonucleic acids (RNAs), like proteins, exhibit a diverse range of secondary and tertiary structures that give rise to characteristic features in Raman and ROA spectra. Although far fewer ROA spectra have been reported for RNAs than for proteins, these indicate a similar level of sensitivity to structure and dynamics. In Fig. 3, we present as an example the Raman and ROA spectra of a 37 nucleotide RNA fragment from Domain I of the encephalomyocarditis virus (EMCV) internal ribosome entry site (IRES) RNA,[23] which guides internal, non-cap dependent, initiation of EMCV protein translation. Most ROA bands observed in the range ~950 to 1150 cm^{-1} originate from vibrations in the sugar–phosphate backbone. Of particular note is a negative–positive–negative triplet at

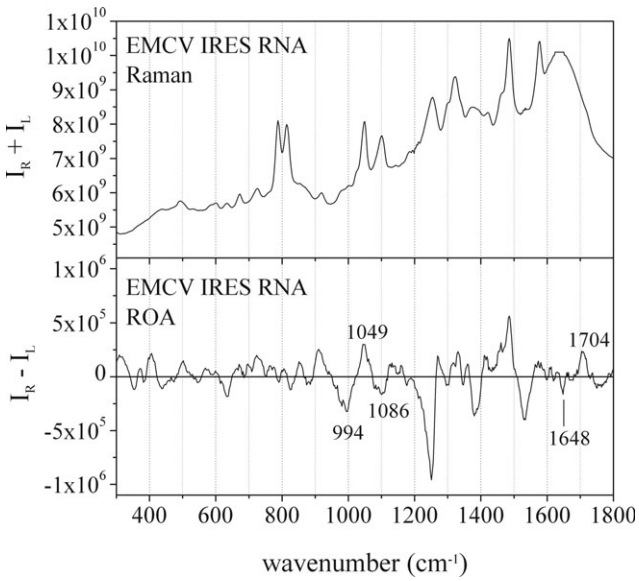

Fig. 3 Backscattered Raman ($I_R + I_L$) and ROA ($I_R - I_L$) spectra for EMCV IRES RNA.

~994, 1049 and 1086 cm^{-1} which has been observed for a number of RNAs and is associated with the C3′-*endo* ribose sugar pucker present in A-form double helices. The intensity of this feature has been shown to be particularly sensitive to the conformational mobility of constituent bases.[23] Within the range ~1648 and 1704 cm^{-1} the broad negative–positive ROA couplet also appears to be indicative of A-type helix although other structural factors may affect this feature.

3. Surface enhancement of ROA

The sensitivity of ROA spectra to the details of secondary and tertiary structure of proteins and nucleic acids has generated significant interest and promoted the expansion of the technique. However, ROA scattering is still orders of magnitude weaker than conventional Raman scattering so necessitating higher sample concentrations and longer data acquisition times. The arguments in favour of the application of plasmon resonance enhancement to Raman spectroscopy hold equally for their application to ROA spectroscopy. It is not surprising that several Raman and ROA spectroscopists have independently attempted to explore this new technique of surface enhanced Raman optical activity, or SEROA. In the following sections, we will discuss these studies on SEROA, which have also highlighted the challenges faced. Recent experimental studies conducted in the authors' laboratories and developments in the theoretical treatments of SEROA have resulted in a better understanding of polarized light scattering from molecules in the vicinity of metal surfaces. Therefore, we will also relate recent work to optimize protocols for reliable SEROA measurements through characterization of the corresponding SERS spectra. We will begin with an examination of theoretical modelling of the SEROA effect.

3.1. Theoretical treatments of SEROA

Efrima first suggested that surface enhancement of ROA spectra was feasible and that it could be informative on the local electric fields and field gradients generated by the plasmon resonances.[8] In this first paper, Efrima considered the effects of large electric field gradients on the electric dipole–magnetic dipole and electric dipole–electric quadrupole and predicted that the values of CIDs may greatly increase, possibly to the order of unity, under these conditions. Efrima also surmised that SEROA spectra should appear very different to the ROA spectra in bulk solution due to the effects of the plasmon resonance on the tensorial contributions to ROA scattering and to the anisotropic environment of the analyte–colloid interface and the local dielectric properties. Although measuring SEROA spectra has proven more difficult than Efrima, and later others, predicted he did raise the first recommendation for caution in interpreting SEROA spectra. Though this was specifically in terms of the possible responsible mechanism, subsequent studies have indeed shown that the analysis of measured SEROA spectra requires care.

In a second paper, Efrima[9] developed this model to include the polarization state of light reflected from an imperfect metal surface and the nature of the electric field close to the metal surface in greater detail. Changes in direction of the local field and the simple magnitude of the electric field were shown to be

not sufficient by themselves to generate large CID values, but that large field gradients are required for this to occur. These field gradients were proposed to be far larger than for the radiative field.[8] This implies that even if the electric field associated with a plasmon resonance is insufficient in intensity to generate a large SERS signal it may still generate measurable SEROA. Efrima derived the following relationship between CID values for the bulk, *i.e.* conventional and non-resonant, ROA experiment (Δ_b) and the surface enhanced ROA experiment (Δ_s):

$$\frac{\Delta_s}{\Delta_b} \approx \frac{[(E_{loc}/d)/E_{loc}]}{[(E_i/2\pi\lambda)/E_i]} \quad (20)$$

where E_i is the incident electric field, E_{loc} is the local contribution to the electric field, d is the range of the local field and λ is the wavelength of radiation.

The effect of reflection from metal surfaces was considered as it has been long established that this process can change the polarization state of circularly polarized light to the elliptically polarized state, that is a linearly polarized component is introduced. This could be a factor particularly for measurements made using SCP or DCP-type ROA spectrometers. Efrima concluded that in the case of imperfect metal surfaces, such as a metal colloid, a significant degree of circular polarization is likely to exist in the beam.[9] However, it is also possible that under such circumstances any linear polarization that might arise could lead to significant artefacts being introduced into measured spectra and which would have to be carefully controlled. Efrima remarked that the magnetic field component was not expected to make a large contribution to SEROA,[9] unlike the situation of ROA in solution, and that near the metal surface only the electric polarizability–electric polarizability contribution was likely to be significant. Efrima also found that the other requirement for the generation of large SEROA signals was either a phase difference between the electric field and its gradient, or a significant imaginary component to the electric polarizabilities of the analyte on the surface.

No further work on modelling ROA responses in the vicinity of metal surfaces was reported until almost a decade later when Hecht and Barron considered, in two papers, the case of a pure electric dipole surface ROA mechanism and included anti-symmetric polarizability components for the first time.[10,11] By considering incoherent scattering from a chiral molecule attached to an isotropic surface fixed with respect to the laboratory frame and with averaging of the ROA tensor products over two dimensions, the authors showed that CID values much larger than those found for ROA measurements in bulk solution may be possible. Hecht and Barron found that these surface CIDs originate from interference between absorptive and dispersive electric dipole–electric dipole molecular polarizability tensor components, and will only be observable under resonant or preresonant conditions. These authors also pointed out that the isotropic surface ROA vanishes for achiral molecules and would give signals of equal magnitude but opposite sign for two enantiomers. If one considers a plane containing the normal to the metal surface and one of the axes parallel to the surface, then a reflection across this plane changes the sign of off-diagonal components in the polarizability tensor. For chiral molecules this reflection generates an enantiomeric isotropic surface but an identical surface for achiral molecules. Hecht and Barron also noted that although some achiral point groups may exhibit chiral projections on a surface these would not be expected to give ROA from isotropic surfaces due to cancellation of enantiomeric projections, though surface ROA could arise from an ordered surface.

A further two decades followed before Janesko and Scuseria[12] introduced full orientational averaging and dressed molecular response tensors for backscattered SCP ROA, though their formalism is applicable to all other ROA experimental configurations. They considered the fields produced by the multipoles induced in a molecule by an oscillating light wave, and the response they would generate in the metal substrate, to specify the multipole moments of the molecule substrate system. Janesko and Scuseria derived expansion coefficients for these multipole moments and so elucidated general selection rules and scaling laws for SEROA. For the simplest model system that they considered, a dipolar sphere, the authors found that predicted SERS intensities agreed well with the literature and that SERS enhancements for vibrational modes whose polarizability derivatives are parallel to the surface normal are 16 times larger than for those modes whose polarizability derivatives are parallel to the surface, in agreement with other workers.[9,24] Furthermore, they also found that SEROA intensity scales with respect to an order parameter and that there were no SEROA contributions to lower than first order of this parameter for full orientational averaging. This is in contrast to the earlier model proposed by Efrima,[9] and results in CID values smaller than those for ROA of bulk samples.

Janesko and Scuseria extended their model to quadrupolar spheres as substrates, and found that for such systems CID values could be considerably increased due to a gradient enhancement mechanism across the metal substrate particle as opposed to across the molecule.[12] The maximum CID using this model was of the order 10^{-2}, and these could be even higher for more realistic substrate models. Dressed ROA tensors were all found to contain contributions from the molecular polarizability, giving SEROA scattering that scales purely as the mean polarizability. This is similar to the chiral surface effect considered earlier by Hecht and Barron,[10,11] and, as with the earlier work, was predicted to be non-zero only for chiral molecules. The model developed by Janesko and Scuseria predicts differences between ICP and SCP ROA spectra, in common with ROA measured under resonance or near resonance conditions with an excited electronic state of the molecule, possibly due to differences in the molecular response to the incident and scattered fields.[25] Dipolar nanorods were also investigated as substrates for SEROA experiments, and again the introduction of quadrupole responses to the model indicated that CIDs could be enhanced.

Shortly thereafter, Bour[26] reworked this multipole electromagnetic field expansion model into a matrix formalism. Bour computed SEROA spectra of CHFClBr for the cases of a single colloidal sphere as substrate, between two colloidal spheres and between four chirally arranged colloidal spheres. Large variations were found between computed SEROA

bands, both in sign and intensity. Thus the modelled SEROA spectral profiles were highly sensitive to changes in analyte–colloid and colloid–colloid interactions, far more so than the corresponding SERS spectra. Bour confirmed that quadrupolar contributions, as well as increasing the number of colloidal spheres around the analyte, increased CID values.

Also of note is recent work by Etchegoin *et al*.[27] modelling polarization effects in SERS. These authors found that the local electric field of the plasmon resonance has a large effect on the polarization state of both the incident and scattered waves and that this needs to be considered for both experimental design and spectral interpretation. Analysis of the effect of the relative orientation of the dimer hot spot with respect to the angle of incidence of the light wave indicated that large enhancement factors for SEROA measurements were not likely. Etchegoin *et al*. also caution that measurement of SEROA could require differentiation between small signals from the analyte molecule and large background signals.

Theoretical models of SEROA are expected to develop quickly in the next few years as polarized spectroscopies are becoming a mainstream field of research and the sophistication of computational methods is now suitable to the task. Such models will continue to be informative and they will provide a basis for interpretation of experimental results, which can otherwise be difficult.

3.2. Experimental studies on SEROA

The measurement of SEROA spectra has proven challenging due to factors already alluded to by the theoretical models, but progress is now being made. Two instances of this phenomenon were reported in the 1990s[28,29] but the signal-to-noise level in each case was low and so the results were not convincing. More recently, a report claimed observation of the SEROA effect for achiral adenine molecules on silver colloids,[30] with the authors attributing the observed signals to surface-induced chirality. However, the bands observed in this study appear likely to have originated in birefringent artefacts rather than authentic SEROA as the performance characteristics noted for the ROA spectrometer used indicate artefactual CID values larger than 10^{-3}, the maximum CID value expected in conventional ROA. Such errors can occur from misalignments of the polarization optics in ROA spectrometers. Similar observations of apparent SEROA signals have been made in a number of laboratories since the first attempts to measure this effect and indicate the challenges involved. It is expected that equal numbers of mirror-image chiral surface domains would form from an achiral analyte,[10,11] leading to zero SEROA in such a case, and emphasising the importance of studies on chiral analytes in order to confirm the reliability of observed SEROA spectra.

Considerable care must be exercised in the analysis of measured SEROA spectra. We present in Fig. 4 relevant spectra measured for proline. In the top two panels are shown the conventional Raman and ROA spectra collected for a 0.939 M solution, with 700 mW of laser excitation at 532 nm and 81 minutes of data collection. In Fig. 4 are also shown the SERS spectra measured for 8.8 mM proline in the presence of both citrate-reduced and hydroxylamine-reduced silver

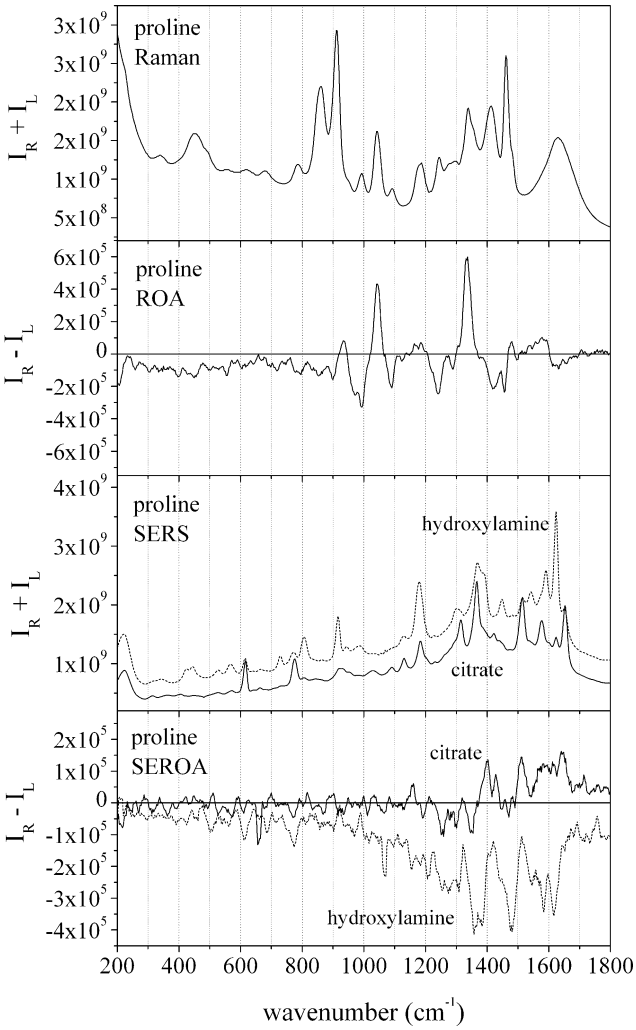

Fig. 4 Backscattered Raman (top), ROA (second), SERS (third) and SEROA (bottom) spectra measured for proline. SERS and SEROA spectra are shown for both citrate- (solid line) and hydroxylamine- (dashed line) reduced colloids. All traces display raw spectra in order to illustrate the effects of artefacts on the SEROA features measured.

colloids with 20 mM K_2SO_4 used as an aggregating agent for both sols. Measurements on similar K_2SO_4 aggregated, citrate-reduced Ag colloids found that they displayed average hydrodynamic diameters spanning the range 800–1200 nm stable for over 2 h, whereas initial hydrodynamic diameters were 200–800 nm (data not shown). These SERS spectra clearly contain different band profiles compared to the Raman spectrum due to both the surface enhancement of specific bands from proline and the presence of bands from the aggregating colloids. Corresponding SEROA spectra measured for proline are shown with 100 mW laser excitation at 532 nm and 60 minutes of data acquisition. These are the raw data and show that there are a number of bands common to both SEROA spectra, in the range $\sim$1300–1550 cm^{-1}, and indicating possible SEROA bands arising from the analyte. The CID values of these SEROA features appear to be of the order 10^{-3}–10^{-4}, and very similar to those measured for the conventional ROA of proline. It is apparent that there are significant differences between the features displayed in the

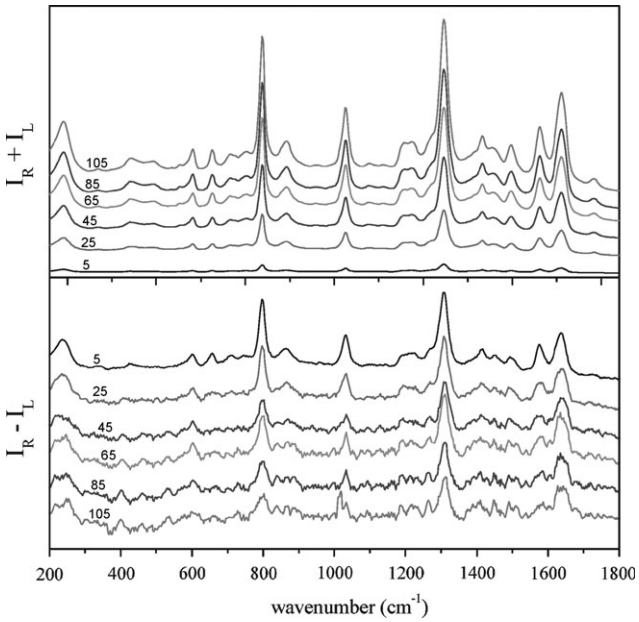

Fig. 5 Backscattered SERS (upper) and SEROA (lower) spectra measured for cytidine using citrate-reduced colloids, measured at the following time intervals: 5 minutes, 25 minutes, 45 minutes, 65 minutes, 85 minutes and 105 minutes. SERS intensities increase with time whereas SEROA features associated with large SERS bands, and therefore prone to artefacts, become less intense, revealing weaker features in the SEROA spectra.

ROA and SEROA spectra, as Efrima originally suggested from the first theoretical model.[8] There are also obvious differences between the two SEROA spectra. The SEROA spectrum measured for the hydroxylamine-reduced colloids is distorted in a negative direction in comparison to the SEROA spectrum measured for citrate-reduced colloids, leading to distortion of several features, particularly the two negatively signed bands appearing near 1600 cm^{-1}. Similar distortions can arise in conventional ROA spectra from polarized Raman bands. As has been already mentioned,[27] the polarization effects induced by plasmon resonances may be significant and should be considered when evaluating SEROA spectra.

The effects of polarizable SERS bands on SEROA spectra can also be observed for the nucleoside cytidine in Fig. 5. SERS spectra for cytidine (at 5.8 μM, 75 mW laser excitation, 3.5 minutes data acquisition per spectrum, citrate-reduced silver colloids and 3.8 mM NaCl aggregating agent) are shown at time intervals of 20 minutes. The SERS spectral profile is consistent throughout this time period with five of the most prominent bands originating in different structural features of cytidine all changing proportionally (analysis not shown). However, greater changes are obvious in the corresponding SEROA spectra shown in the lower panel in Fig. 5, as aggregation proceeds presumably due to the varying effects of plasmon resonances on the polarization states of incident and scattered waves as predicted by Etchegoin *et al.*[27] Several apparent SEROA bands, originating from intense SERS bands, appear to decrease in relative intensity, indicating that these bands are probably artefacts and are being averaged out over time. After ~45 minutes several weak SEROA bands begin to appear; such as those at ~400, 1270 and 1460 cm^{-1}, suggesting that these weak features may originate from the cytidine analyte. We note that this behaviour is similar to that predicted by Etchegoin and co-workers[27] and illustrates that the stability of colloids over time periods longer than those typically used in conventional SERS needs to be characterized. Although the SEROA spectra presented in Fig. 4 and 5 are not definitive proof of the SEROA technique, they do illustrate the importance of characterization of SEROA bands and how these can vary with time and the aggregation behaviour of colloids.

A single SEROA study of a chiral pentapeptide, enkephalin, has been reported.[31] Since then, several studies have been reported on proteins, by the same group, who showed that the sensitivity of SEROA is conditioned by optimization of the concentration of the analyte, colloid and aggregating agent composing the sample.[32]

In Fig. 6, the intensity of two resonance SERS peaks for myoglobin using 532 nm are plotted as a function of concentration of myoglobin (Fig. 6a), Ag colloids (Fig. 6b) and NaCl (Fig. 6c), respectively. The two peaks, being the symmetric (solid line) at 1374 cm^{-1} and anti-symmetric (dashed line) (1169 cm^{-1}) ν(pyr half-ring) stretching modes, were chosen to monitor SERS intensity as they were found to be independent of the signal-to-noise ratio, which originates mainly in fluorescence. The results clearly show a dependence of SERS intensity on variation of the sample concentration conditions. The optimum conditions, *i.e.* the best SERS spectrum of Mb was achieved at 10^{-7} M myoglobin, 70% Ag and 0.1 M NaCl, as it is shown in Fig. 7a.

It is worth mentioning that, while the number of molecules per unit volume is important when measuring Raman spectra, the number of molecules currently adsorbed at SERS active sites influences the detected intensity in SERS spectra. This explains the intensity behaviour observed in Fig. 6, in which, as the sample concentration initially increases, the number of SERS active sites will also increase, and consequently higher SERS intensity will be obtained. This response will continue until a maximum limit has been reached, beyond which any increase in the sample concentration will yield a decrease in SERS intensity due to an increase in the background or/and increased fluorescence, which results from the sol aggregating, leading to an increase in opacity, especially in the case of coloured samples like myoglobin.

Resonance enhancement of Raman scattering (RRS) occurs when an electronic transition is triggered by the incident light. The electronic excitation increases the Raman scattering probability of vibrational normal modes in the spatial vicinity of the chromophore, so enhancing these signals. When RRS enhancement couples with surface plasmon enhancement, a further enhancement of the resonant vibrations occurs, known as surface enhanced resonance Raman scattering (SERRS). Therefore, the SERS measurement for myoglobin at 532 nm shown in Fig. 7a is actually a SERRS spectrum. SERRS measurements are, of course, only possible when there is sufficient overlap between the electronic transition frequency of the sample and the surface plasmon resonance of the nanoparticles. In extension of the terminology described above, measurement of ROA under electronic resonance

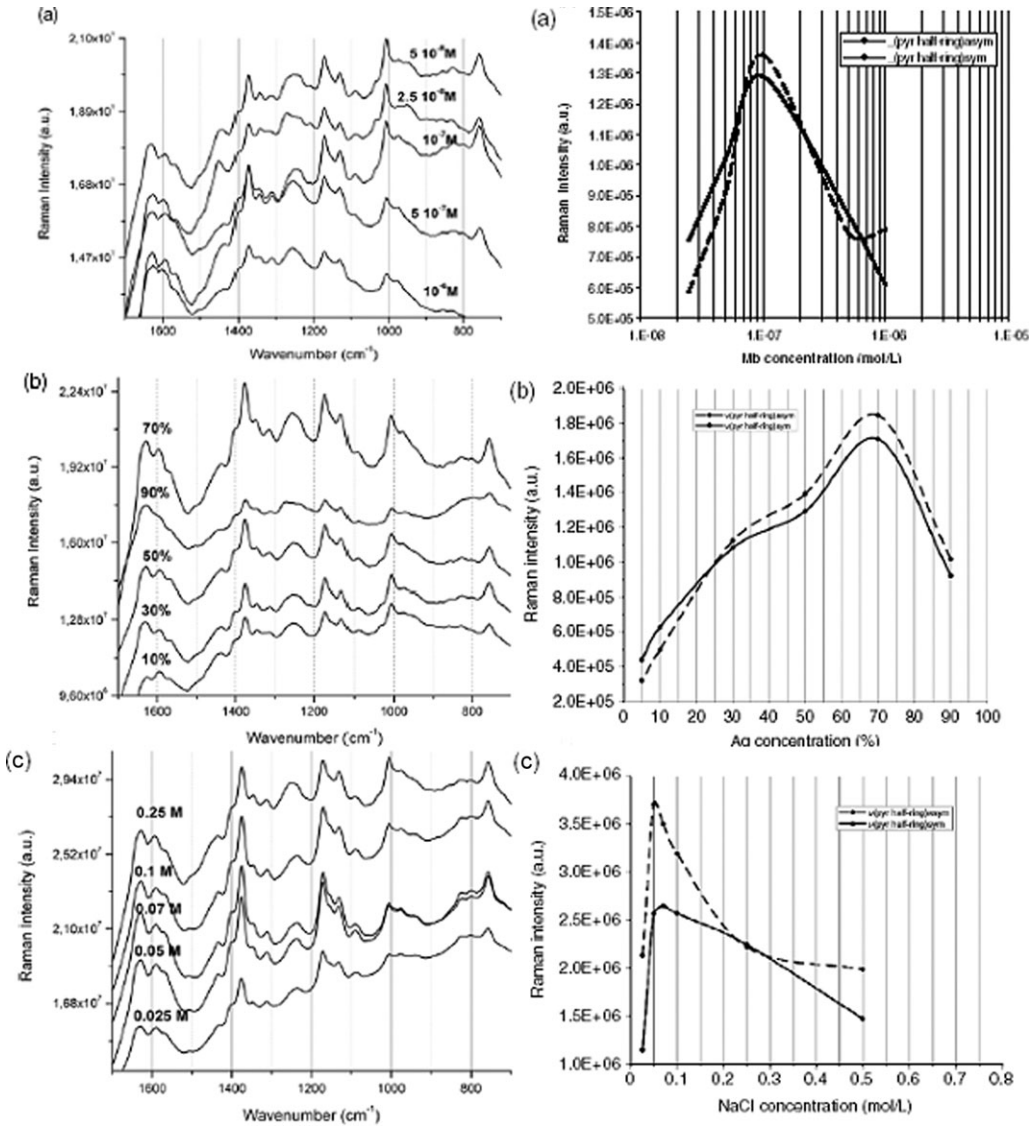

Fig. 6 Intensity of two SERRS peaks: symmetric ν_4 (solid line) and anti-symmetric ν_{30} (dashed line) of ν(pyr half-ring) at 1374 cm^{-1} and 1169 cm^{-1}, respectively, plotted as a function of myoglobin concentration (a), Ag concentration (b), and NaCl concentration (c).[32]

conditions leads to resonance ROA (RROA), and the combination of electronic resonance with SEROA generates resonance SEROA (SERROA).

The RROA and SERROA spectra of myoglobin at 532 nm are also shown in Fig. 7b and c, respectively, with the SERROA measurement being carried out under the optimized conditions mentioned above. Chiral peaks in the spectrum were observed after only a few minutes but, in order to achieve a better signal-to-noise ratio, the measurement was performed for 5 minutes. The SERRS signal was simultaneously monitored for erratic hot-spots and was found to be stable during the experiment. In order to verify the authenticity of the surface enhanced effect, a RROA spectrum of myoglobin of 100 μM concentration was also recorded, as shown in Fig. 7b, which was acquired over no less than 32 h in order to achieve a sufficient signal-to-noise ratio. Comparing the RROA and SERROA spectra in Fig. 7, it is noticeable that the chiral signals of myoglobin, labelled with corresponding frequencies, are similar in both spectra. In particular, the region 1300–1400 cm^{-1}, which also exhibits the largest signal enhancement in the SERRS spectrum, has a considerable signature overlap around 1395, 1353, 1321 and 1299 cm^{-1}. The SERROA peak around 1353 cm^{-1} appears to have bigger FWHM than the corresponding RROA feature, which may explain the absence of bands at ~1366 and 1344 cm^{-1}. All Raman bands in this region have previously been assigned for the RRS spectrum,[33,34] and have been shown to be enhanced by the resonance Raman effect at the laser excitation used, 532 nm.[35] At the sample concentration used of 100 μM, conventional ROA bands from polypeptide backbone vibrations would be too weak to measure, so the peaks found in the RROA spectrum in Fig. 7 are assigned to the resonance enhancement of the porphyrin vibrations. Addition of the colloids and aggregation agent, NaCl, leads to further enhancement of SERS and SEROA bands and to a combination of resonance and surface enhancement of chiral signals.

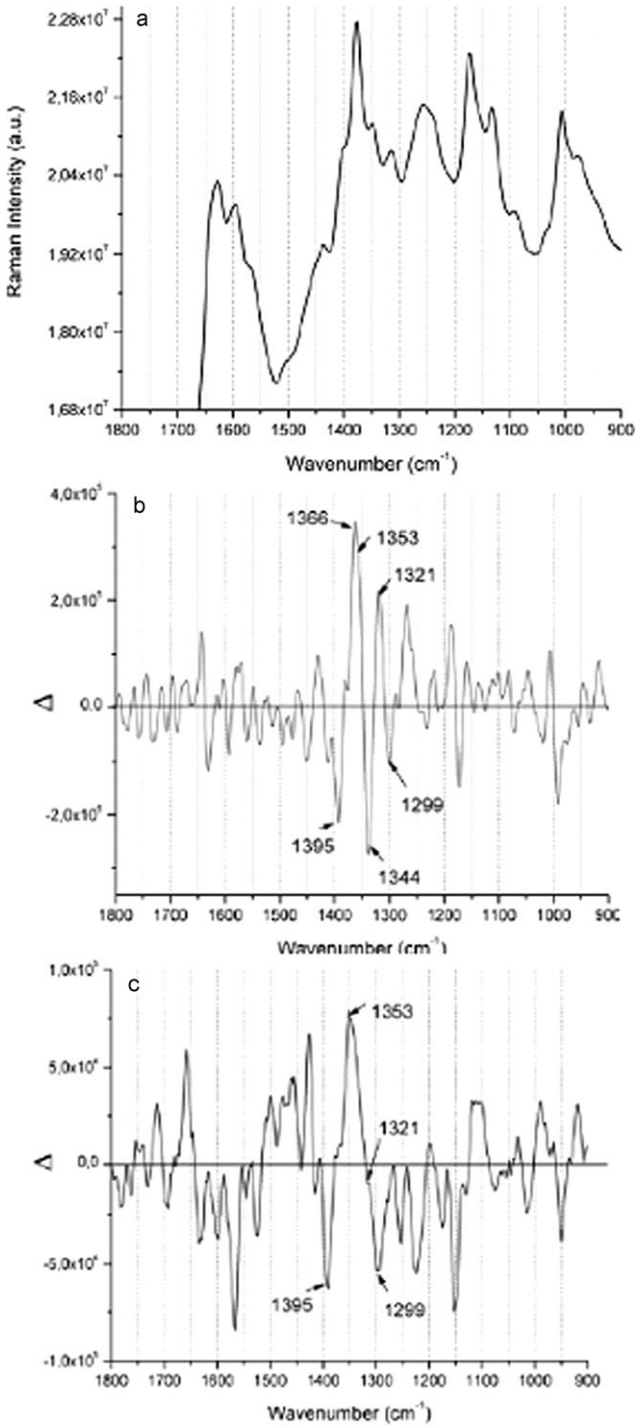

Fig. 7 SERS (a), RROA (b) and SERROA (c) spectra of myoglobin, measured under optimized conditions from Fig. 6, *i.e.*, 10^{-7} M myoglobin, 70% Ag and 0.1 M NaCl.[32]

Abdali *et al.* have also recently reported the SERRS and SERROA spectra of another porphyrin-containing protein, cytochrome c.[36] The RRS, RROA, SERRS and SERROA spectra of cytochrome c are shown in Fig. 8a–d, respectively. RROA features observed for cytochrome c are unlike those typically observed for globular proteins, indicating that the chiral signals measured originate in vibrations of the porphyrin ring. In the range 1100–1700 cm^{-1}, most of the RRS bands

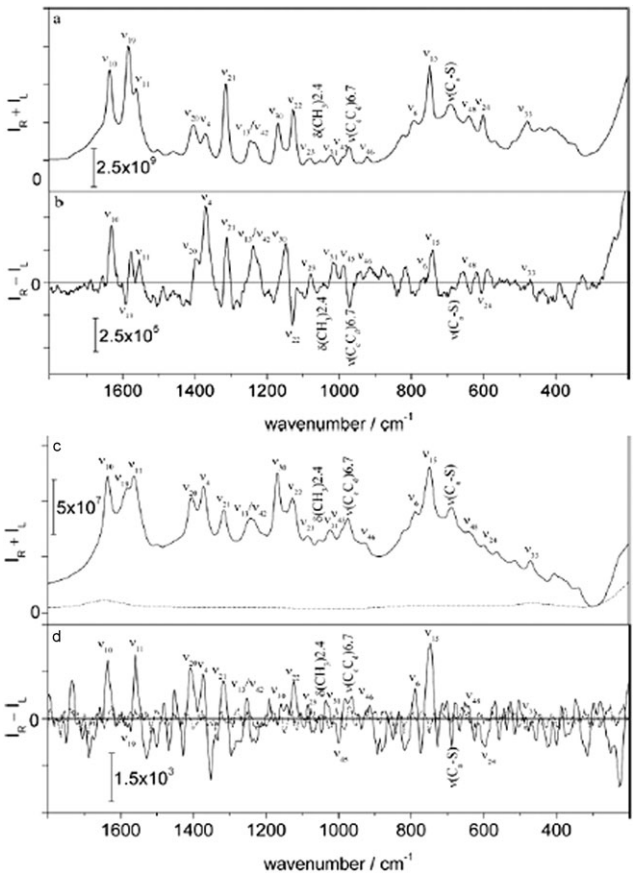

Fig. 8 Resonance Raman (a), ROA (b), SERRS (c) and SERROA (d) spectra for cytochrome c.[36] Control SERRS and SERROA spectra for colloid in the absence of cytochrome c are shown as dotted lines.

observed for cytochrome c are assigned to strongly enhanced in-plane vibrations that also give rise to contributions for the major features in the RROA spectrum shown. While the ν_{10} and ν_{11} transitions have positive resonance ROA, the ν_{19} signal, located between these vibrations, appears to be a negative–positive couplet, indicating contributions from two transitions. A comparison of the resonance ROA spectra of cytochrome c and myoglobin strongly suggests that the observed signals are from the porphyrin group in a chiral environment.[32]

In-plane transitions can be assigned to the bands ν_{20} and ν_4, both of which exhibit positive ROA. Interestingly, the predominant feature of this region of the spectrum is due to ν_4, a transition whose resonance enhancement is highly sensitive to the excitation wavelength, not being very strongly enhanced by the Q-band excitation caused by the 532 nm laser employed in the measurement. It appears that the collective half ring stretching vibration responsible for the ν_4 signal is highly chiral, resulting in a strong signal. Between 800 and 1100 cm^{-1}, a number of less enhanced signals can be assigned to local in-plane vibrations, deformations and side chain vibrations with correspondingly weak ROA contributions.[36] Notable exceptions are the two overlapping bands assigned to ν_{45} and the propionate stretching vibration at $\sim$974 cm^{-1}, which appear as a positive–negative couplet in the RROA spectrum. The strongly enhanced ν_{15} is the main feature of the

wavenumber region below 800 cm^{-1}, again giving rise to a positive RROA signal, whereas the remaining signals in the region exhibit limited or no ROA.

The RRS and SERRS spectra for cytochrome c, shown in Fig. 8a and c, respectively, are remarkably similar. Other than a slight fluorescence background in the SERRS spectrum, the main differences between the RRS and SERRS spectra are: the selective surface plasmon enhancement of transitions ν_{10} and ν_{11}, almost concealing ν_{19}; the stronger enhancement and inversion of intensity relation of ν_{20} and ν_4 compared to ν_{21}, and the inversion of intensity relation of ν_{30} and ν_{22}. The spectrum of a negative control sample, prepared by replacing protein with water, is also presented (dotted line in Fig. 8c). The SERROA spectrum of cytochrome c, Fig. 8d solid line, retains several of the main features of the RROA spectrum (Fig. 8b), while the dotted line represents, analogous to the SERRS spectrum in Fig. 8c, the negative control spectrum for a mixture of only colloids and water, which also shows the so-called noise level of the measurement. It is worth noticing that there is some degree of correlation between the enhancements of Raman active transitions in SERRS and the corresponding SERROA signals. In the wavenumber region above 1100 cm^{-1}, the peaks corresponding to the ν_{10} and ν_{11} transitions reproduce the positive signals found in the RROA spectrum, whilst the ν_{19} couplet is decreased to the noise level. In addition to the fact that this transition appears to be less enhanced by the plasmon effect compared to the two other transitions, the lack of a SERROA signal may also be due to an increased polarization of the transition (or transitions) resulting in artefact prone data collection. The ν_{20} SERROA signal is in good agreement with the RROA, whereas the ν_4 SERROA signal is considerably less enhanced in comparison to other peaks in this region. This feature is rather interesting, as the SERRS spectrum of cytochrome c shows a favourable enhancement of the ν_4 transition compared to ν_{20}, while the RROA band from ν_4 is pronounced, an effect that is apparently reversed in the SERROA spectrum.

Other significant differences can be observed between the RROA and SERROA spectra, seen in Fig. 8b and d, respectively, of cytochrome c for a number of bands, including the loss of the ν_{30} band for the SERROA measurement, possibly due to changes in the dipole moment and polarization of the molecule when adsorbed to the silver colloids or from symmetry changes in the porphyrin. The full inversion of the SERROA ν_{22} band also indicates a possible symmetry inversion in the prosthetic group. This change is even more pronounced when examining the weak couplet, assigned to the overlap of ν_{45} and the propionate stretching vibration at 974 cm^{-1} in the resonance ROA spectrum. Whilst this couplet was positive–negative in the RROA spectrum, the SERROA spectrum reveals a weak negative–positive couplet, the negative portion of the couplet commencing immediately after ν_{31}. In addition to being an interesting contribution to the overall understanding of plasmon effect and the influence on adsorbed molecules to metal surfaces, the inversion of these bands also shows how cautious one must be when using ROA spectra to assign spectral features in SERROA spectra. Janesko and Scuseria[12] found that quadrupolar responses of the substrate may significantly enhance ROA in certain cases, which could explain the apparent lack of SERRS signal from ν_{21}, as the SERROA signal is enhanced.

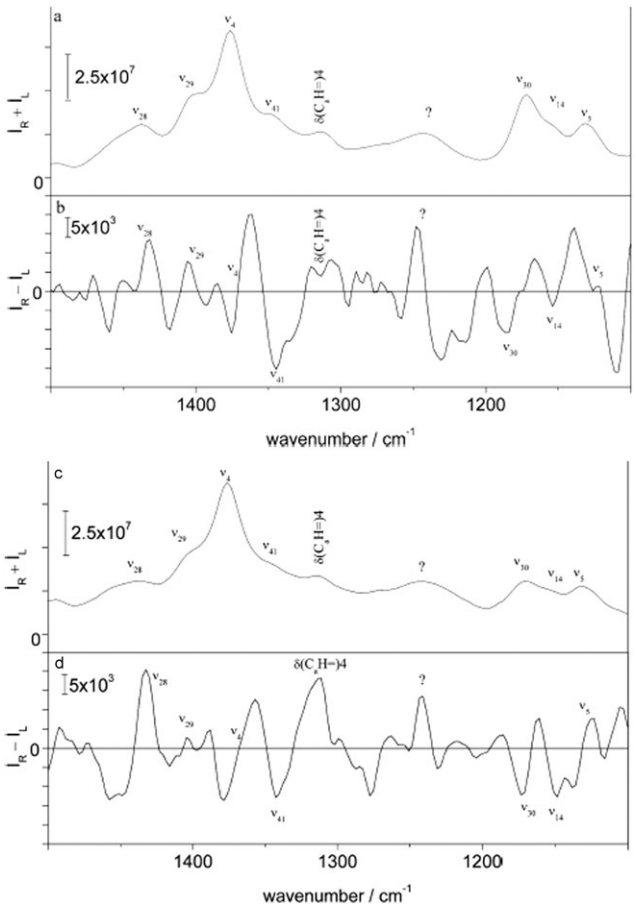

Fig. 9 SERRS (a) and SERROA (b) spectra for myoglobin, and SERRS (c) and SERROA (d) spectra for the myoglobin–azide complex.[37]

The sensitivity of SERROA has also recently been used to investigate ligand binding by myoglobin.[37] SERRS and SERROA spectra of Mb are shown in Fig. 9a and b, respectively, while SERRS and SERROA spectra of the myoglobin–azide complex are shown in Fig. 9c and d, respectively. No significant differences can be seen when SERRS spectra of Mb and Mb + azide are compared, whereas larger differences are apparent in their corresponding SERROA spectra, seen in Fig. 9b and d. This demonstrates that the sensitivity to structural perturbations inherent to ROA spectroscopy is retained in SERROA. The ν_{28} couplet is not wavenumber shifted upon binding of the azide ion, and it is believed that the normal mode responsible for ν_{28}, a C_α–C_m stretching mode, is not strongly influenced by ligand binding. The corresponding SERROA signals, together with signals due to ν_{41} and the vinyl in-plane bending mode at 1305 cm^{-1}, represent the main porphyrin signature in the myoglobin spectra. In the SERROA spectrum, the ν_4 transition can be assigned to a negative–positive couplet and the negative contribution following this feature to ν_{41}, also originating from a symmetric half-ring stretching vibration. In the region 1200–1400 cm^{-1}, wavenumber shifts can be observed in addition to changes in intensity ratios by ligand binding, indicating structural

changes in the porphyrin. Upon binding of azide to the porphyrin, the couplet assigned to ν_4 broadens by 8 cm^{-1}, blue shifting the negative contribution whilst red shifting the positive contribution. As a result, the SERROA signals assigned to ν_{41} and the vinyl in-plane bending mode appears to be slightly red shifted, taking into account that the noise observed in the myoglobin spectrum does not allow for unambiguous peak intensity assignment. This broadening of the porphyrin SERROA signature may indicate structural changes in the porphyrin upon complexation of the azide.

Although spectral changes occur in the RRS spectra of myoglobin above 1500 cm^{-1} upon complexation of azide, only a few SERROA band changes were found,[37] suggesting that the localized porphyrin transitions found in this region are less susceptible to chiral analysis. However, it should be emphasised that the structural changes induced by complexation of azide or other small ligands in porphyrin-containing metalloproteins are very small (less than 0.5 Å), and cannot be determined directly by X-ray diffraction. Therefore, the ability of SERROA to detect these structural changes is highly promising for future work in this direction.

4. Conclusions

The measurement of the SEROA effect has proven a challenge since it was first proposed, though recently SEROA spectra have been reported for biological molecules. This success shows that SEROA has considerable potential as a new chiroptical probe of molecular structure and molecule–surface interactions. The original rationale for investigating SEROA was to increase the sensitivity of the relatively weak ROA effect and so extend its applicability to biological samples at much lower concentration. As SEROA is still a very new technique it is not yet clear how readily applicable it will be to all biological molecules, but current and future studies will answer this question. We note that considerable care should be taken to optimize experimental parameters in order to minimize spurious signals or other artefacts. Furthermore, the SEROA technique still awaits a definitive proof through the measurement of mirror image spectra for enantiomers. It is also not yet clear if the high CID values that have been predicted as being possible will be observed, as the few reliable SERROA spectra so far reported have also been recorded under electronic resonance conditions. Nevertheless, considerable progress has been made in terms of both experimental results and in developing more detailed and insightful theoretical models. Improved theoretical models can be expected to provide further insight into SEROA mechanisms and potentially allow the molecular orientation of an analyte to be determined. As with SERS investigations of analyte–metal interactions, a population of randomly oriented analyte molecules may be expected to yield a composite spectrum from their individual SEROA contributions, though with these individual contributions also being sensitive to conformational heterogeneity. It is possible that molecular orientation of an analyte on a metal surface can change with time and, though this is being examined with SERS, SEROA band patterns may be expected to be particularly sensitive to such reorientation events as chiroptical band patterns cancel out for opposite stereochemistries. Although this behaviour is likely to complicate SEROA measurements, with careful optimization of experimental conditions it also suggests a new method for probing the dynamic behaviour of analyte–metal interactions. Alternatively, it may be possible to control such behaviour through ordered samples, such as in Langmuir–Blodgett films, engineered nanostructures or three dimensional nanoparticle arrays, and so stabilize SEROA signals.

New techniques often lead to unexpected applications or scientific advances and it is still too early to confidently predict the future impact of SEROA. However, the work reported to date has highlighted several avenues of research that warrant investigation. Experiments have only been conducted for a small number of analyte molecules but the combination of electronic resonance mechanisms with the surface plasmon resonance enhancement, in the form of SERROA, has so far proven more successful than measurements of SEROA. The SERROA strategy may also allow detailed comparisons of the two enhancement mechanisms and serve as a novel probe of metalloprotein structure. Ligand binding analysis by SERROA may develop into an extremely powerful method in the future, as a more solid understanding of the signals associated with this surface plasmon enhanced differential spectroscopy is achieved. Understanding and recognising prosthetic group SERROA signatures could be combined with *ab initio* calculations as the porphyrin signals observed appear to be only weakly dependent on the surrounding protein structure, and calculations restricted to the active site should produce reliable results.

SEROA intensities measured to date are low and whether this is due to the chemical enhancement effect rather than the electromagnetic effect, which is strongly dependent on the polarization, is a matter of speculation. Future research on this question may be informative for developing a better understanding of SERS mechanisms in general. The anticipated extension of SEROA experiments to the NIR frequency domain will allow use of more stable gold nanostructured substrates, potentially making experiments easier and more reliable. At the very least, SEROA spectra measured using gold and silver surfaces could provide complementary approaches to developing the technique. As the number of reliable SEROA spectra increases, we will then be better placed to assess their usefulness as spectral fingerprints for different types of biological molecules, as sensitive probes of structural changes and as monitors of chiral surface–analyte interactions.

Acknowledgements

EB would like to thank Miss Alison Hobro and Miss Nicola Yaffe for their assistance in preparing this review and for providing unpublished data, Miss Sylvia Pilorz for providing unpublished data, EPSRC (GR/S75727/01) and RSC (GR/T05554/01) for research funding and the National Physical Laboratory (NPL) for material support. Christian Johannessen, Jesper Nygaard, Peter White and Thomas Nørbygaard are acknowledged for their collaboration in the work on SERROA for myoglobin and cytochrome c. The Danish

National Research Foundation is also acknowledged for its financial support to SA.

References

1 L. D. Barron, *Molecular Light Scattering and Optical Activity*, Cambridge University Press, Cambridge, 2nd edn, 2004.
2 W. Hug, in *Handbook of Vibrational Spectroscopy*, ed. J. M. Chalmers and P. R. Griffiths, Wiley, New York, 2002, vol. 1.
3 M. Fleischmann, P. J. Hendra and A. J. McQuillan, *Chem. Phys. Lett*., 1974, **26**, 163.
4 D. L. Jeanmaire and R. P. Van Duyne, *J. Electroanal. Chem*., 1977, **84**, 1.
5 M. G. Albrecht and J. A. Creighton, *J. Am. Chem. Soc*., 1977, **99**, 5215.
6 S. Nie and S. R. Emory, *Science*, 1997, **275**, 1102.
7 K. Kneipp, Y. Wang, H. Kneipp, L. T. Perelman, I. Itzkan, R. R. Dasari and M. S. Feld, *Phys. Rev. Lett*., 1997, **78**, 1667.
8 S. Efrima, *Chem. Phys. Lett*., 1983, **102**, 79.
9 S. Efrima, *J. Chem. Phys*., 1985, **83**, 1356.
10 L. Hecht and L. D. Barron, *Chem. Phys. Lett*., 1994, **225**, 525.
11 L. Hecht and L. D. Barron, *J. Mol. Struct*., 1995, **348**, 217.
12 B. G. Janesko and G. E. Scuseria, *J. Chem. Phys*., 2006, **125**, 124704.
13 P. W. Atkins and L. D. Barron, *Mol. Phys*., 1969, **16**, 453.
14 L. D. Barron and A. D. Buckingham, *Mol. Phys*., 1971, **20**, 1111.
15 L. D. Barron, M. P. Bogaard and A. D. Buckingham, *J. Am. Chem. Soc*., 1973, **95**, 603.
16 W. Hug, S. Klint, G. F. Bailey and J. R. Scherer, *J. Am. Chem. Soc*., 1975, **97**, 5589.
17 L. D. Barron, L. Hecht, I. H. McColl and E. W. Blanch, *Mol. Phys*., 2004, **102**, 731.
18 E. W. Blanch, L. Hecht and L. D. Barron, *Methods*, 2003, **29**, 196.
19 W. Hug and G. A. Hangartner, *J. Raman Spectrosc*., 1999, **30**, 841.
20 L. A. Nafie and D. Che, *Adv. Chem. Phys*., 1994, **85**, 105.
21 L. A. Nafie, B. E. Brinson, X. Cao, D. A. Rice, O. M. Rahim, R. K. Dukor and N. J. Halas, *Appl. Spectrosc*., 2007, **61**, 1103.
22 L. D. Barron, L. Hecht, E. W. Blanch and A. F. Bell, *Prog. Biophys. Mol. Biol*., 2000, **73**, 1.
23 A. J. Hobro, M. Rouhi, E. W. Blanch and G. L. Conn, *Nucleic Acids Res*., 2007, **35**, 1169.
24 M. Moskovits, *J. Chem. Phys*., 1982, **77**, 4408.
25 L. D. Barron and J. R. Escribano, *Chem. Phys*., 1985, **98**, 437.
26 P. Bour, *J. Chem. Phys*., 2007, **126**, 136101.
27 P. G. Etchegoin, C. Galloway and E. C. Le Ru, *Phys. Chem. Chem. Phys*., 2006, **8**, 2624.
28 S. Higuchi, N. Ikoma, T. Honma and Y. Gohshi, in *Proceedings of the Twelfth International Conference on Raman Spectroscopy*, ed. S. R. Durig and J. F. Sullivan, Wiley, Chichester, UK, 1990.
29 G.-S. Yu, PhD thesis, Syracuse University, USA, 1994.
30 H. Kneipp, J. Kneipp and K. Kneipp, *Anal. Chem*., 2006, **73**, 1363.
31 S. Abdali, *J. Raman Spectrosc*., 2006, **37**, 1341.
32 S. Abdali, C. Johannessen, J. Nygaard and T. Norbygaard, *J. Phys.: Condens. Matter*, 2007, **19**, 285205.
33 A. Hu, K. M. Smith and T. G. Spiro, *J. Am. Chem. Soc*., 1996, **118**, 12638.
34 N. Engler, A. Ostermann, A. Gaussmann, D. C. Lamb, V. E. Prusakoc, J. Schott, R. Schweitzer-Stenner and F. G. Parak, *Biophys. J*., 2000, **78**, 2081.
35 A. R. Bizzari and S. Cannistrato, *Appl. Spectrosc*., 2002, **56**, 1531.
36 C. Johannessen, P. White and S. Abdali, *J. Phys. Chem. A*, 2007, **111**, 7771.
37 C. Johannessen and S. Abdali, *Spectroscopy (Amsterdam, Neth.)*, 2007, **21**, 143.

